Medical & Biological Engineering & Computing
https://doi.org/10.1007/s11517-020-02205-w

ORIGINAL ARTICLE

Design and implementation of a novel wireless modular capsule robotic system in pipe

Jian Guo [1] · Zihong Bao [1] · Qiang Fu [1] · Shuxiang Guo [1,2]

Received: 8 October 2019 / Accepted: 23 May 2020

Abstract

Capsule endoscopy is a new type of technology in the diagnosis and treatment of digestive diseases, with painless and low invasive features. However, current capsule robots have many problems, such as over-sized, single function and lack of active locomotion control. This study proposed and designed a new wireless modular capsule robotic system in pipe. The modular capsule robots could move forward and backward in the pipe in the axial direction, turn in a bending environment, and achieve the rendezvous and separation action through the three-dimensional rotating magnetic field generated by the three-axis Helmholtz coils. In this paper, the drive system of the three-axis Helmholtz coils, the power supply control system, and the modular capsule robot structure were analyzed and designed respectively. Finally, a series of characterization experiments were carried out to evaluate the motion characteristics of the modular capsule robots, including the influence of the flow environment imitated to human body's gastrointestinal motility, the frequency of the input signal, and the different structure of the robots on the movement characteristics of the modular capsule robot in this study. The study also evaluated the turning characteristics of robots. Experimental results showed that under different circumstances, modular capsule robots had good motion characteristics, and the effectiveness of the modular functionality had also been verified.

Keywords Modular interface · Three-axis Helmholtz coils · Capsule robot · Power supply control system

1 Introduction

In recent decades, with the progress of science and technology, wireless capsule endoscopic robots become an effective alternative to traditional endoscopic techniques [1]. Compared with the traditional endoscopic technology, wireless capsule endoscopy has many advantages [2]. The size of wireless capsule endoscopes is smaller than the traditional endoscopic, is easy to check, and has less impact on patients' normal working life. The ideal capsule endoscopy robots need to be responsible for gastrointestinal tract detection and treatment. Due to the small internal space, capsule robots need to integrate various sensors and microcontrollers into multiple functions, Therefore, a number of key technologies of wireless capsule robots are still to be solved.

At present, various research institutes focus on the research of wireless capsule robots in two directions: one is the study of their active movement [3–5], the other is the study of the image acquisition of robots and other additional features, such as image enhancement, robot positioning, delivery of drugs, and tissue collection [4, 6–9].

The medical technology company Given Imaging from Israel introduced the world's first commercial capsule endoscopy product, named M2A capsule [10]. But its movement relied on the physiological natural peristalsis of the digestive tract, which means it is a passive motion. Yim and Sitti at Carnegie Mellon University in the USA designed a prototype of a magnetically actuated soft capsule endoscope [11–13]. Through the external magnetic field, this mechanism could proactively deform to compress the chamber in the body and release the medicine. In the following study, they designed a device for biopsy based on the original drug delivery robot

✉ Qiang Fu
fuqiang6369@hotmail.com

✉ Shuxiang Guo
guoshuxiang@hotmail.com

1 Tianjin Key Laboratory for Control Theory & Applications in Complicated Systems and Biomedical Robot Laboratory, Tianjin International Joint Research and Development Center, Tianjin University of Technology, Binshui Xidao, Tianjin 391, China

2 Faculty of Engineering, Kagawa University, 2217-20 Hayashi-cho, Takamatsu 760-8521, Japan

Published online: 24 July 2020

which uses microgrippers to collect tissue samples. Kim and Ishiyama at Tohoku University proposed an active locomotion robot with targeted drug release based on a rotating magnetic field control of a three-axis Helmholtz coil system [9]. The robot solved the problem of active locomotion and drug delivery of the capsule robot at the same time. However, the robot has less capacity for movement and less drug-carrying capacity. Yan et al. from Shanghai Jiao Tong University in China designed an expanding extending robotic endoscope with spiral legs [14, 15]. This robot could crawl imitating the geometer moth. However, its movement speed is slower than that of a spiral capsule robot. Zhang et al. of Dalian University of Technology conducted continuous research on magnetic wireless capsule robots and developed a variable-diameter capsule robot based on multiple wedge effects and a dual hemisphere capsule robot [16–21]. When the variable-diameter robot rotates, the thrust generated by the multi-wedge effect through the wedge gap promotes the axial movement of the robot to realize the non-contact movement of the robot. The dual hemisphere capsule robot can take the active and passive modes of flexible movement. In recent years, Guo Lab of Kagawa University conducted an in-depth study of an active-motion capsule robot driven by a three-axis Helmholtz coil [22–26]. The lab proposes a hybrid robot that can switch between two modes of motion and is more adaptable. The Biomedical Robot Laboratory of Tianjin University of Technology also conducted continuous research on medical micro-pipeline robots and developed a spherical medical microrobot [27, 28]. The robot used a spherical shape structure and it was more space efficient. This design effectively reduced the size of the robot and provided more flexibility in movement. The advantages and disadvantages of the above robots are shown in Table 1.

Although some achievements have been made in the research of wireless capsule robots in pipe, the research in this field is still in the stage of continuous exploration and improvement for clinical application, and a series of key technical problems still need to be solved urgently. On the one hand, the large size of capsule robots may lead to poor movement characteristics and also result in low practicality of the capsule robot. On the other hand, the features of the wireless capsule robots are relatively simple, and functions such as image acquisition, drug delivery, and biopsy cannot all be integrated on the single robot. In view of the above problems, this paper proposed and designed a wireless modular capsule robot system in pipe. The spiral modular capsule robots of this system were driven by the universal rotating magnetic field and could realize the rendezvous and separation control between the modular capsule robots.

This paper is structured as follows. Firstly, we elaborated on the overview of the modular capsule robot system in pipe. Secondly, we proposed the structure and prototype of the modular capsule robots. Thirdly, we carry out the experiments in different environments and verify the modular capsule robots' motion performance. Finally, we give conclusions and future work.

2 System overview

Figure 1 shows the conceptual diagram of the wireless modular capsule robot system in pipe. The system consisted of the master part and the slave part. At the master PC, the doctor manipulated the joystick according to the image and the position information displayed on the screen transmitted from the capsule robot of the slave part. The joystick converted the doctor's operation into position parameters and sent it to the PC. The master PC's power supply control system converted the position parameters into the commands of the power supply of the slave part and then transmitted them to the power supply wirelessly. After receiving the signal, the power supply outputted the corresponding three-phase alternating current to change the rotating magnetic field generated by the three-axis Helmholtz coils. At the same time, it was possible to control the movement of capsule robots with built-in permanent magnets.

2.1 The three-dimensional rotating magnetic field

The Helmholtz coil is made up of two annular coils of exactly the same size and structure. The two coil faces are coaxial and parallel, and the distance between their center points is equal to the radius of the respective loop coil. If a sinusoidal alternating current was passed through the Helmholtz coil, a uniform magnetic field of sinusoidal variation in intensity could be produced in its central region. If two pairs of orthogonal Helmholtz coils were fed with an alternating current having a phase angle of 90° different from each other, a rotating magnetic field plane perpendicular to both coil faces can be superimposed in the central region. However, if we added a pair of Helmholtz coils in this system to form a three-axis Helmholtz coil which is orthogonal to each other and passed a certain form of alternating current in the system, in theory, an arbitrary plane of rotating magnetic field should superimpose on the central area of the coil. This study uses such a three-axis orthogonal circular Helmholtz coil, as shown in Fig. 2; the specific parameters are shown in Table 2.

Zhang et al. proposed a method of adjusting the axial direction of the external rotating magnetic field generated by the three-axis Helmholtz coils [18]. At the same time, there are many research institutions to study the control method of capsule robots by the three-dimensional rotating magnetic field [29, 30]. This approach could provide the safety and reliability that other approaches could not effectively achieve. It had great potential for medical robotic applications and had become a major trend of research in this area.

Table 1 Pros and cons of robots

Robot	Advantage	Disadvantages
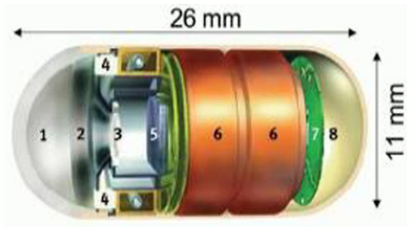 M2A Capsule	Image acquisition function	Passive motion, lack of other functions
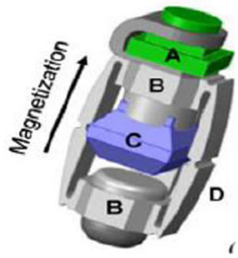 The magnetically actuated soft capsule endoscope	Release the medicine	Passive motion, lack of other functions
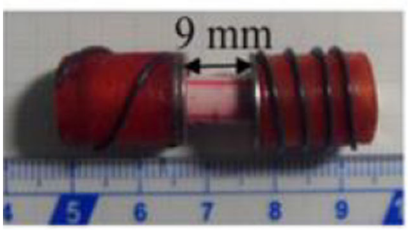 Drug delivery robot	Active locomotion and drug delivery of the capsule robot	Less capacity of movement and less drug carrying capacity
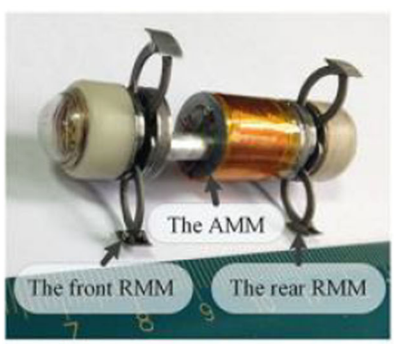 The expanding-extending robotic endoscope with spiral legs	Crawl imitating the Geometer moth	Slower movement speed

Table 1 (continued)

 The variable-diameter capsule robot	The non-contact movement	Lack of other functions
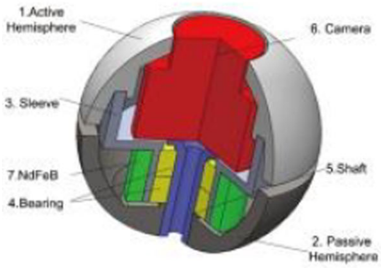 The dual hemisphere capsule robot	Active and passive modes of flexible movement, Image acquisition function	Too large
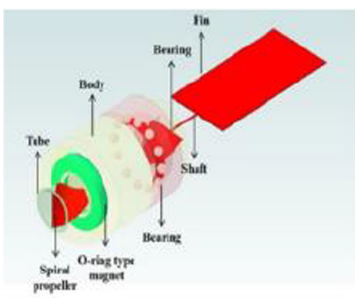 The active-motion capsule robot	Active-motion, switch between two modes of motion	Lack of other functions
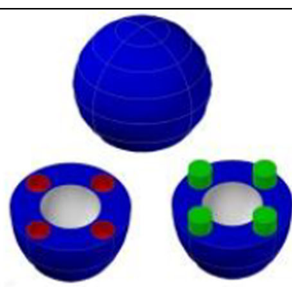 The spherical medical micro robot[	Provided more flexibility in movement	Lack of other functions

Figure 3 shows the schematic diagram of the three-axis Helmholtz coils used in this paper. Take the center point of the three Helmholtz coils as the origin o, the outer ring coil axis as the x-axis, the middle ring coil axis as the y-axis, and the inner ring coil axis as the z-axis, to establish a space rectangular coordinate system $oxyz$. $\vec{n}$ is the normal vector of the

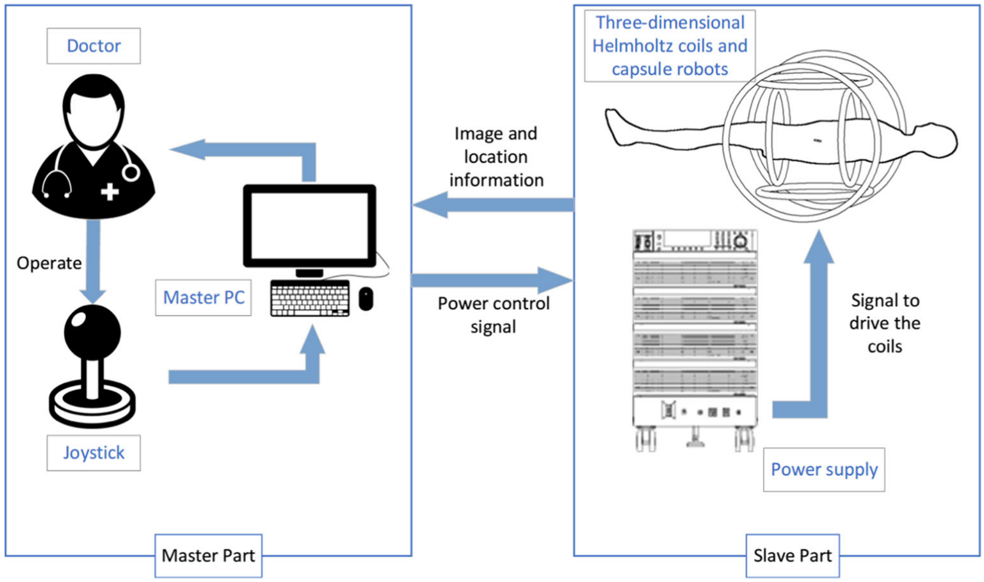

Fig. 1 The conceptual diagram of the wireless modular capsule robot system in pipe

plane of the rotating magnetic field. As shown in the figure, the angles between it and the x-axis, y-axis, and z-axis are α, β, and γ, respectively.

As long as the three-axis Helmholtz coil is fed with the current of the following equation to drive the coil to generate a plane normal vector and the direction of the vector space rotating magnetic field:

$$\begin{cases} I_x = -I_0 \sin\alpha \sin(\omega t - \varphi_x) \\ I_y = -I_0 \sin\beta \sin\left(\omega t + \varphi_y\right) \\ I_z = I_0 \sin\gamma \sin(\omega t) \end{cases} \quad (1)$$

Fig. 2 The three-axis orthogonal circular Helmholtz coils

where α, β and γ are the angle between the vector $\vec{n}$ and the x-axis, y-axis, and z-axis angle, respectively; $\tan\varphi_x = \frac{\cos\beta}{\cos\gamma\cos\alpha}$;$\tan\varphi_y = \frac{\cos\alpha}{\cos\gamma\cos\beta}$; I_0 is the amplitude of the currents; ω is the angular frequency of the sinusoidal alternating current.

According to Eq. (1), passing current into the coils could produce a rotating magnetic field with a normal vector $\vec{n}$. However, this formula only applied to the first quadrant of the Cartesian coordinate system. In order to solve this problem, the alternating current fed into each coil needed to be processed separately in the opposite phase. By combining these processes, it is possible to achieve control of the rotating magnetic field in space on each quadrant and coordinate axis. According to Eq. (1) and its variants, we could get the rotational direction of the rotation magnetic field and the directions of the normal vectors in eight quadrants in the Mathematica. Figure 4 shows the results, which is basically consistent with the formula description.

2.2 The power supply control system

This study used the Kikusui PCR3000LE2 three-phase AC power supply as a three-axis Helmholtz coil drive source. It

Table 2 The specific parameters of the three-axis Helmholtz coils

Coil	Wire diameter (mm)	Turns	Radius (mm)	Resistance (20 °C) (Ω)
X-coil	1.8	216	294.3	5.52
Y-coil	1.8	174	211.4	3.29
Z-coil	1.8	126	157.4	1.86

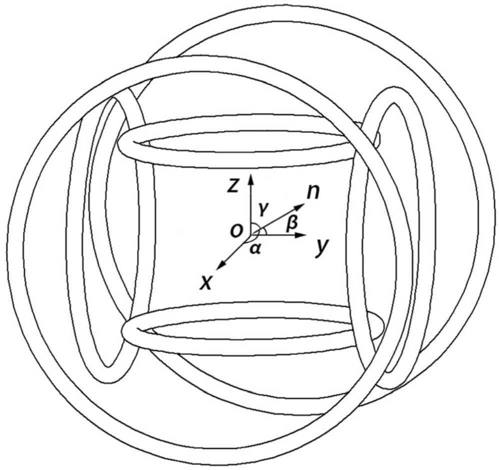

Fig. 3 The schematic diagram of the three-axis Helmholtz coils

could output any adjustable three-phase alternating current signal enough to satisfy the needs of the system for a three-dimensional rotating magnetic field. And the magnetic field could effectively drive the capsule robot movement in the human gastrointestinal tract. In this study, a highly customized power supply control system had been developed for this power supply to realize its complicated control. The doctor could order the direction of the robot's movement through the joystick. After receiving the instruction, the power supply control system converted the coordinate information sent from the joystick into a corresponding power control signal, and then wirelessly transmitted it to the power supply. Then, the power supply would output the corresponding drive signal to the three-axis Helmholtz coils. At the same time, the power status information would be fed back to the power supply control system and displayed on the interface.

Figure 5 shows the power supply control system interface. The interface is divided into four parts. The top of a column is the device list information bar. The second part is the tab bar. This part is used to display the control mode tab page. Figure 5 a shows the axial control tab interface and Fig. 5 b shows the 3D control tab interface. The third part is the control status bar. This part is used to display the control status of the joystick and power output. The bottom column is the power status information bar, where the real-time display of the power connection, the output status information, voltage information, and frequency information, allowing users to keep abreast of the latest power status.

3 The proposed modular capsule robots

3.1 Design and fabrication of modular capsule robots

The modular capsule robotic system designed in this paper is shown in Fig. 6. The system concludes two main units: the guide and the auxiliary robot. Both capsule robots have a built-in permanent magnet which magnetized in the radial

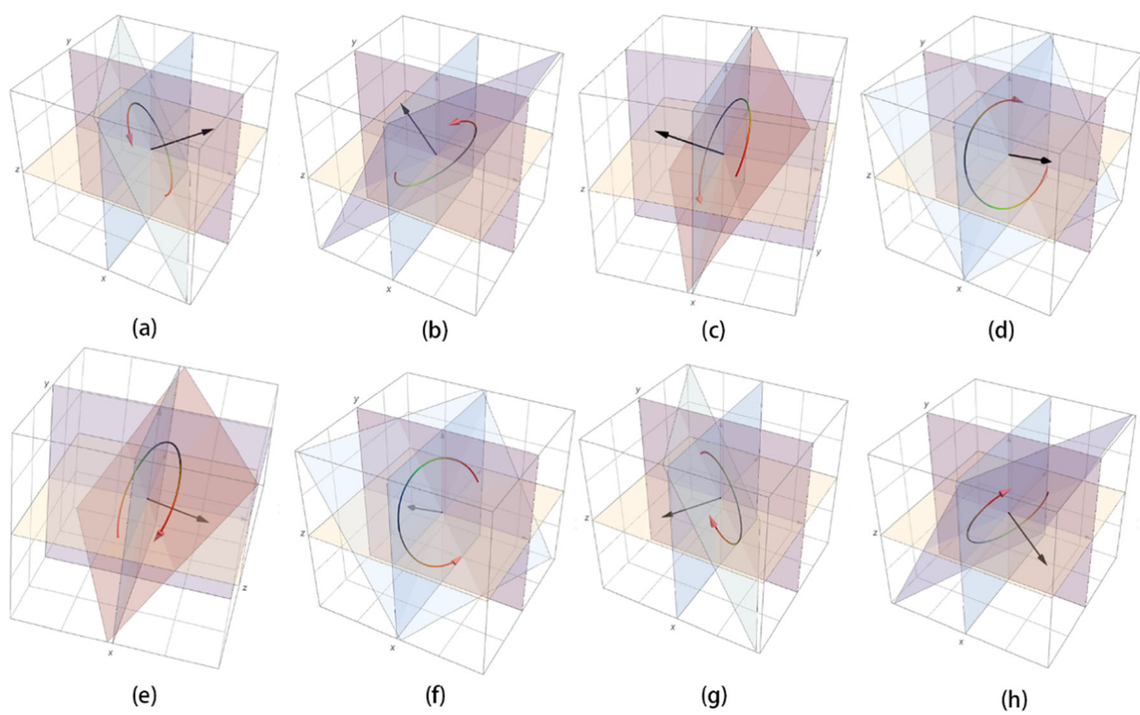

Fig. 4 The rotating magnetic field simulation results for each quadrant. **a** First quadrant. **b** Second quadrant. **c** Third quadrant. **d** Fourth quadrant. **e** Fifth quadrant. **f** Sixth quadrant. **g** Seventh quadrant. **h** Eighth quadrant

direction and can perform a spiral motion driven by an external rotating magnetic field. At the same time, the robot body can be driven to rotate with its central axis as a rotation axis. And two magnets which are magnetized in the axial direction are placed in the rear of the guide robot and in the front of the auxiliary robot, respectively. These two magnets can be utilized to combine two parts of the robot through the force of different poles of magnets.

Due to size constraints, the robots proposed in this study are not easy to manufacture using traditional machining methods. Therefore, we split a single robotic model into several parts and then used ABS (acrylonitrile butadiene styrene)

Fig. 5 The power supply control system interface. **a** The axial control tab interface. **b** The 3D control tab interface

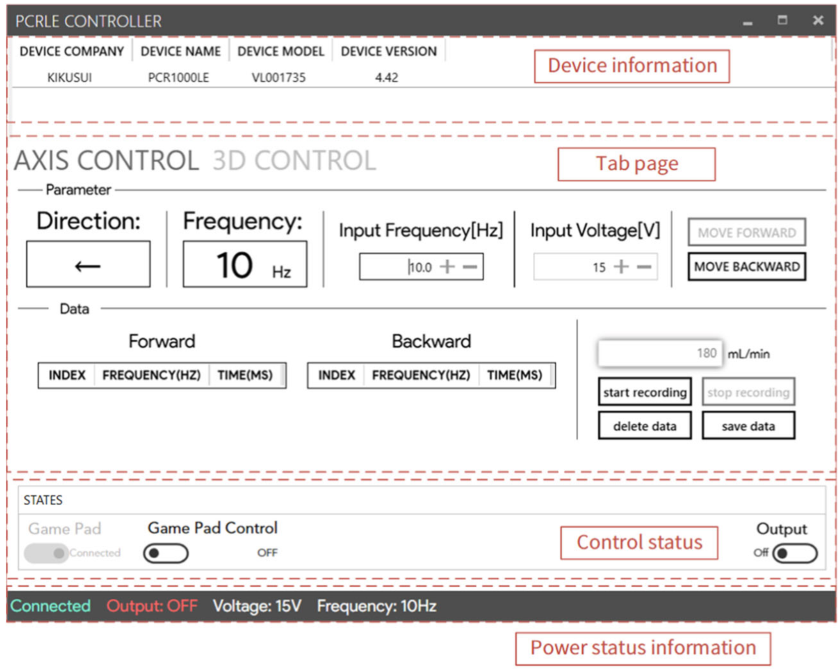

(a) The axial control tab interface

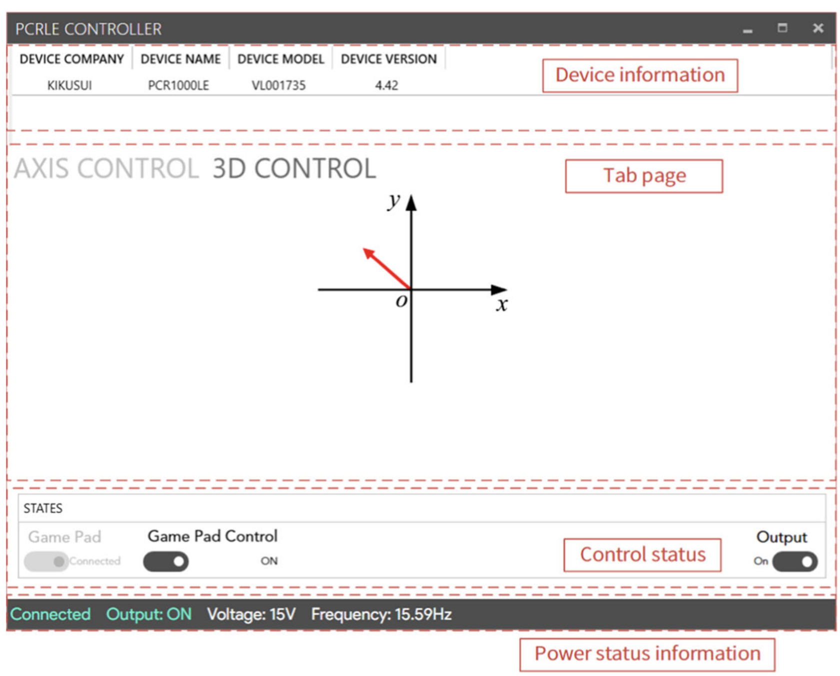

(b) The 3D control tab interface

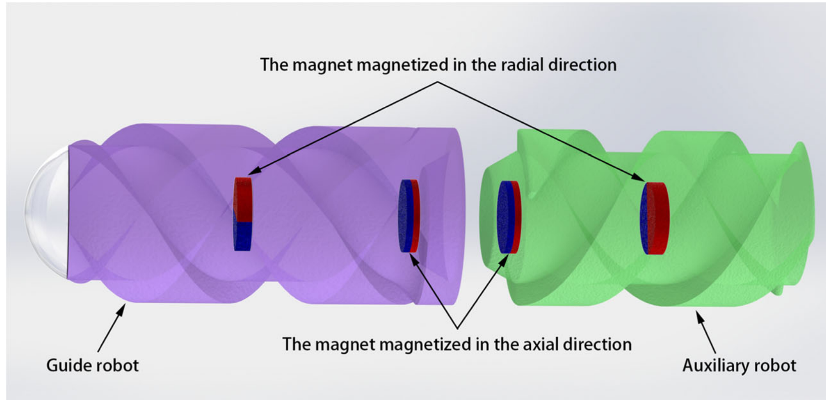

Fig. 6 The 3D model of the modular capsule robots

material to print out each individual part using the 3D printer, as shown in Fig. 7a and then assembled to complete the prototype, as shown in Fig. 7b, c. Table 3 shows the parameters of the robots' prototype [31].

3.2 Principle of modular capsule robots' movement

As described in Section 3.1, the permanent magnets in the center of the two robots which magnetized in the radial direction can be driven by the external rotating magnetic field generated by the three-axis Helmholtz coils. And meanwhile, the robots perform a spiral motion which rotation axis was the center axis under the rotation of the magnet. When it rotates in the liquid and its direction of rotation is counterclockwise, as a result of the reaction force exerted by the liquid flow on its helical guide groove, the guide robot will move forward simultaneously, as shown in Fig. 8.

Similarly, the performance of the permanent magnet which magnetized in the radial direction of the auxiliary modular robot in the rotating magnetic field is consistent with that of the forward robot. But the spiral direction of helical diversion grooves on it is opposite to the guide robot. It is counterclockwise when the sight is from the

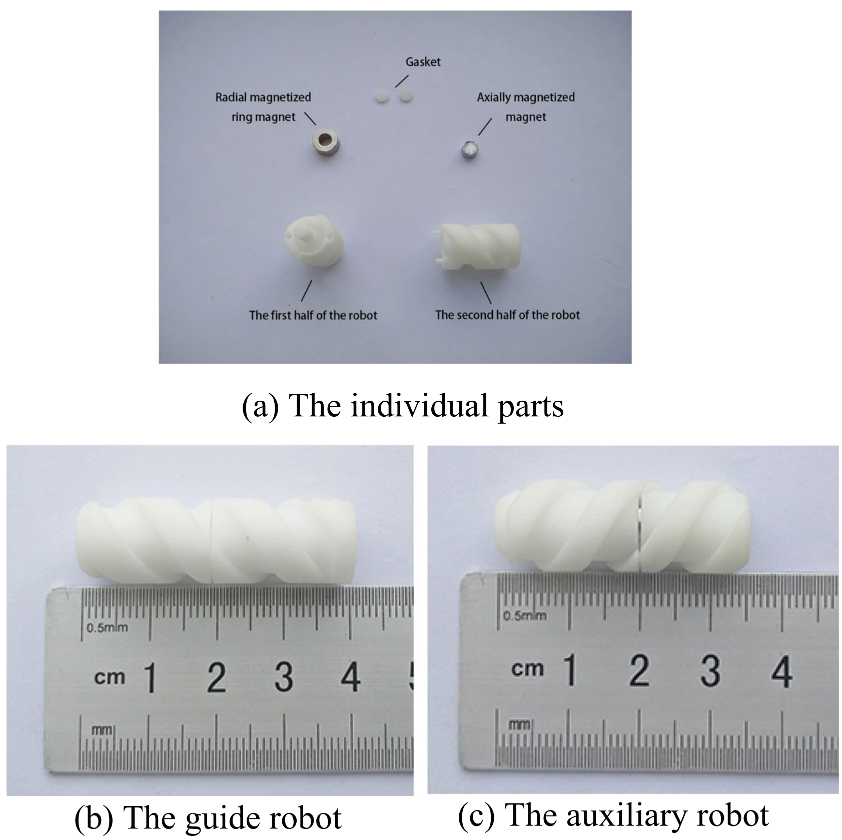

Fig. 7 The prototypes of modular capsule robots. **a** The individual parts. **b** The guide robot. **c** The auxiliary robot

Table 3 The parameters of robots

Coil	Length (mm)	Diameter (mm)	Grooves depth (mm)	Grooves width (mm)	Grooves number (mm)
Guide robot	39.4	12.5	1.5	4.5	2
Auxiliary robot	33.8	12.5	1.5	4.5	2

robot's head to tail. This leads to the fact that its axial direction is opposite to that of the guide modular robot when they are under the same rotating magnetic field, as shown in Fig. 9 [31].

Therefore, the direction of movement of the auxiliary robot and the guide robot is on the contrary under the same rotating magnetic field. Based on this principle, the auxiliary robot can follow and meet the guide robot in the same magnetic field. And it can also be separated after the two robots have docked because of the opposite movement of them [31].

3.3 Design of modular interface of capsule robots

A tapered groove in which the tilt angle is 30° is designed in the rear of the guide robot. And with it is the conical bulge which in the front of the auxiliary robot and its tilt angle is also 30°. So, these two structures can be fitted with each other. The docking interface can be modularized, and in this case, all of the auxiliary robots can dock with the robots which have the guide robot's docking interface.

In order to make two robots docking and keeping the state, there should be a mechanism to attract two robots together. Figure 10 describes the mechanism to achieve this purpose. As is shown in this figure, two permanent magnets which are magnetized in the axial direction are placed in the rear of the guide robot and in the front of the auxiliary robot. Therefore, when the distance between them is close enough, the magnetic force generated between the two magnets will attract the two robots together. The size of the magnetic force between the two magnets when they are docked can be altered as long as adjusting the position of the magnets in the robots.

3.4 Dynamic model of modular capsule robot in fluid environment

With some previous researches [32], a dynamic model of a modular capsule robot in fluid was established and analyzed in this paper. First, let θ be the helix angle of the helical guide groove. The velocity of the surface of the capsule in the circumferential direction U and the velocity V_a in the direction of rotation y and direction x perpendicular thereto can be decomposed when the capsule robot rotates to obtain the velocity component V along the helical direction and the velocity component W perpendicular to the helical direction:

$$\begin{cases} V = U\cos\theta + V_a\sin\theta \\ W = U\cos\theta - V_a\sin\theta \end{cases} \tag{2}$$

Figure 11 shows a schematic cross-sectional view of the robot in a direction perpendicular to the helix. c is the distance from the robot to the pipe, a is the pitch, ha is the height of the spiral guide groove, b is the screw top width.

For easy analysis, only analyze the pressure within one pitch, as shown in Fig. 12.

$$\frac{d}{dx}\left(h^3\frac{dp}{dx}\right) = 6\ \mu\mathrm{W}\frac{dh}{dx} \tag{3}$$

where h is the distance from the surface of the robot to the pipe wall, p is the pressure of the robot surface and the fluid, and μ is the viscosity of the liquid. Integrate Eq. (3) to get:

$$p = 6\ \mu\mathrm{W}\frac{h-h_0}{h^3}x + C_1 \tag{4}$$

where h_0 and C_1 are indefinite values.

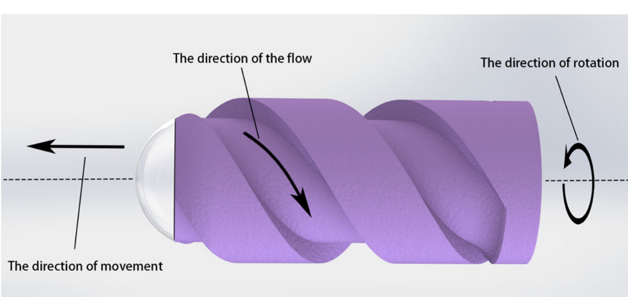

Fig. 8 The rotational motion and axial motion of the guide robot

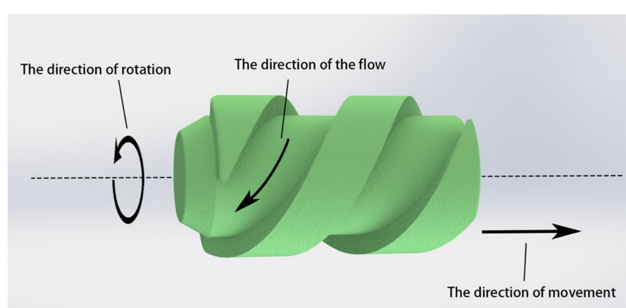

Fig. 9 The rotational motion and axial motion of the auxiliary robot

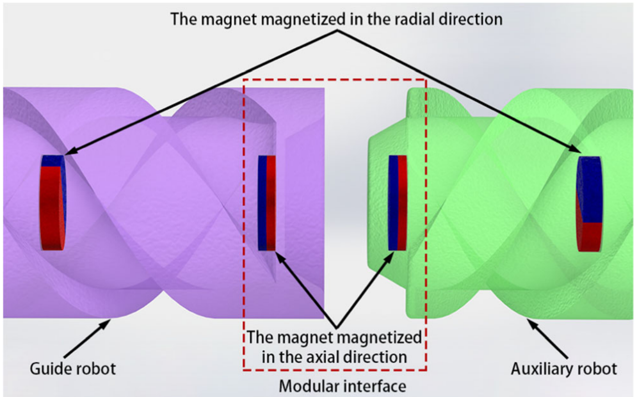

Fig. 10 The modular interface diagram [31]

According to the Navier-Stokes equations, the fluid on the surface of the helical guide groove is analyzed:

$$\begin{cases} \frac{1}{\mu}\frac{\partial p}{\partial x} = \frac{\partial^2 u}{\partial z^2} \\ \frac{1}{\mu}\frac{\partial p}{\partial y} = \frac{\partial^2 v}{\partial z^2} \end{cases} \tag{5}$$

where u is the velocity of the fluid perpendicular to the direction of the helix and v the velocity of the fluid in the direction of the helix.

According to the previous study [33], we can get the axial thrust of the robot Fa:

$$\left\{ \frac{3\beta(1-\beta)\gamma^2[(r-c\gamma)\omega r\sin\theta - V_a r\cos\theta](\omega r\sin\theta - V_a\cos\theta)\cos\theta}{(1-\beta)[(r-c\gamma)\omega r\sin\theta - V_a r\cos\theta] + \beta r(1+\gamma)^3(\omega r\sin\theta - V_a\cos\theta)} \cdot (r-c-c\gamma) - \frac{(1-\beta)(r-c\gamma)}{c(1+\gamma)}\cdot V_a - \beta V_a \right\} \tag{6}$$

where $\beta = \frac{b}{a}$, $\gamma = \frac{h_a}{c}$, $\lambda = \frac{h_a}{r}$, r is the radius of the capsule robot, and L is the length of the capsule robot.

4 Experimental results

In order to verify the performance of the modular capsule robots designed in this study and the effect of the control system, a series of experiments were carried out to evaluate the characteristics of the wireless modular capsule robotic system.

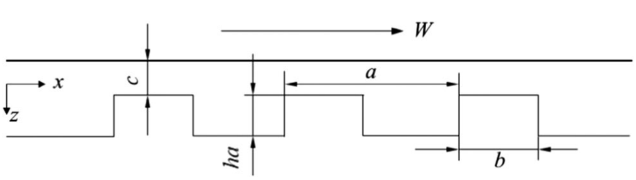

Fig. 11 The schematic diagram of the robot along the direction perpendicular to the helix

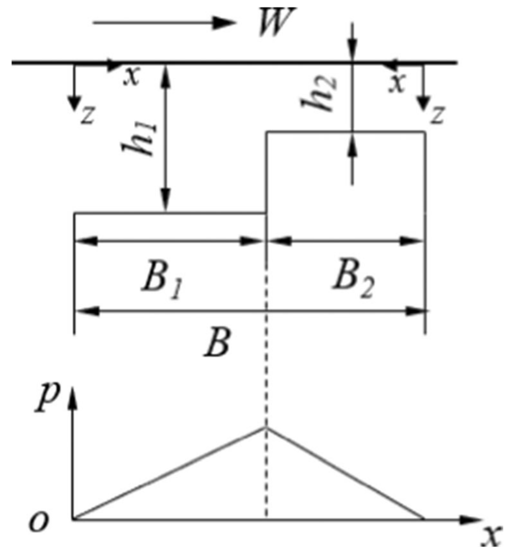

Fig. 12 The profile parameters of a single pitch of the robot

Figure 13 shows the experimental platform. The experimental platform includes the three-axis Helmholtz coils that can generate a rotating magnetic field as described above, the three-phase AC power supply PCR3000LE2 that can be used to drive the coils, the master PC, and the joystick for wireless control. Peristaltic pump simulates the human digestive environment. This study also used a peristaltic pump that can simulate the digestive environment of the human body. Figure 14 shows the elbow diagram.

When the peristaltic pump output flow rate is 180 mL/min, the flow rate of the fluid in the tube is 2 cm/s (the maximum rate of human intestinal peristalsis), so this study chooses 180 mL/min as the maximum output flow rate, and 160 mL/min, 140 mL/min, and 120 mL/min are selected for comparison simultaneously.

First, we evaluated and analyzed the axial forward and backward movement characteristics of the guide and auxiliary robots at different flow rates. Figure 15 shows the relationship between the frequency of the alternating current signal input to the Helmholtz coils and the average moving speed of the guide robot when it moves downstream forward under different flow velocities in the tube. Figure 16 shows the relationship between the current signal frequency and the average moving speed of the guide robot when it moves upstream backward under different flow velocities in the tube.

Figures 15 and 16 show that the guide robot in the modular capsule robot designed in this paper can move normally in the rotating magnetic field. When it moves downstream forward, its starting frequency is 2 Hz and its cutoff frequency is 19 Hz. The cutoff frequency (19 Hz) that means the frequency above which the robot can no longer rotate continuously in synchronous with the rotational magnetic fields. Cut-out frequency is well understood for magnetic helical robots in uniform fields;

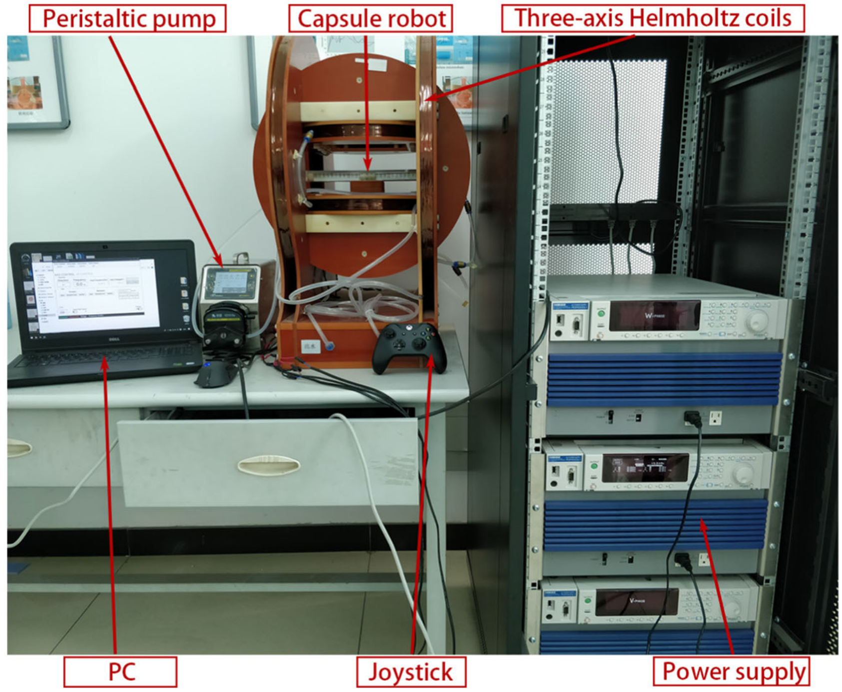

Fig. 13 The experimental platform

it is discussed in our previous researches. The experimental results of the spiral jet motion indicated the linearity between magnetic field changing frequency and the moving speed from 2 to 19 Hz [23].

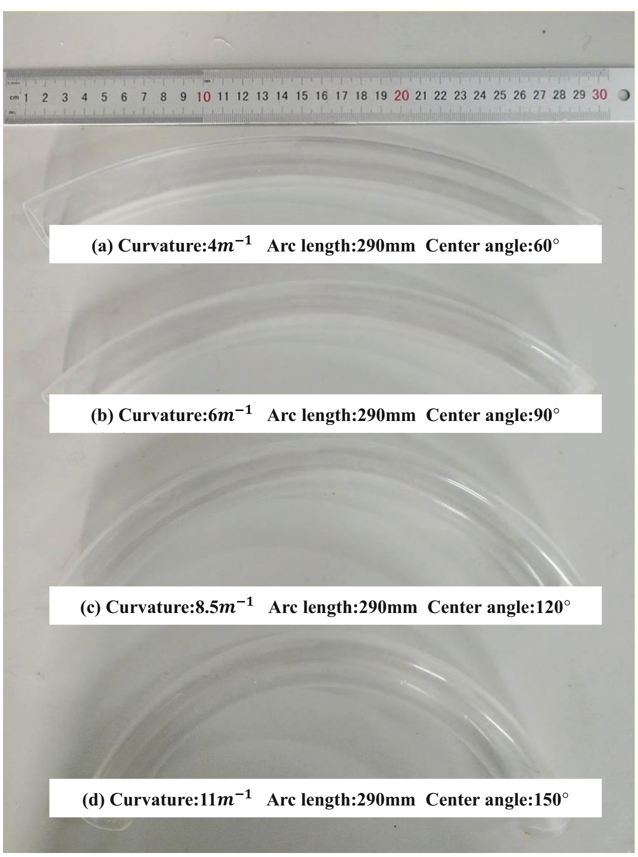

Fig. 14 The elbow diagram

As can be seen from Fig. 16, when the guide robot moves upstream backward, as the water flow rate increases, the starting frequency of the guide robot is greatly reduced, even reaching 16 Hz at the maximum flow rate of 180 mL/min. The reason for this is that the guide robot has a modular interface at the rear of it for docking with the auxiliary robot. The diameter of the interface portion is the same as the diameter of the robot body. This factor causes the interface to block part of the water flow into the guide groove of the robot body when the guide robot moves upstream backward, thereby reducing part of the axial thrust force that the robot can obtain through the rotational movement. As a result, its starting frequency increases drastically as the flow rate increases.

There is a special phenomenon that needs attention. From 11.5–12 Hz, whether it is moving downstream forward or upstream backward, under each flow velocity, the average axial movement speed of the guide robot has a relatively obvious downward trend. Then, as the frequency increases, the robot's speed gradually picks up. This fluctuation occurs because when the robot rotates at a lower frequency, due to the effect of gravity, the guide groove has a longer contact time with the pipe wall. The friction generated by these contact points will provide a great impetus to the robot when rotating. When the robot's rotation frequency increased to a certain value, the body will be wrapped around a circle of fluid film. This layer of fluid film will separate the robot wall from the tube. At this time, the friction between the robot and the pipe wall is reduced, and the propulsion force is provided almost

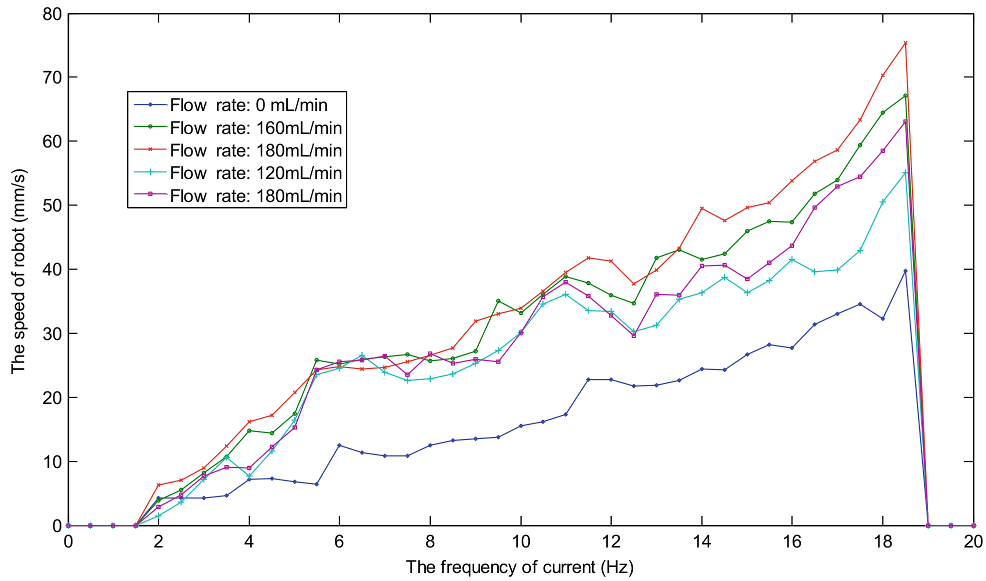

Fig. 15 The relationship between the frequency of the current signal and the average moving speed of the guide robot when it moves downstream forward under different flow velocities

entirely by the shear stress of the fluid on the guide groove. As described above, for the guide robot, the tail part of the modular interface not only has a blocking effect on the water flow behind but also blocks the water flow in front of it. As a result, this interface reduces the amount of propulsion that the water stream provides to it, and the propulsion force cannot maintain the previous robot speed. In the case of downstream forward, the impact of this factor is slight. When the guide robot moves upstream backward, its impact is obvious.

Figures 17 and 18 show the relationship between the current signal frequency and the average moving speed of the auxiliary robot when it moves downstream forward and upstream backward under different flow velocities. It can be seen from the figure that when the auxiliary robot moves forward, the starting frequency and the cutoff frequency are the same as those of the guide robot. When it moves upstream backward, the starting frequency does not increase significantly when the flow velocity increases due to the different structures of the tail with the guide robot. In the working frequency, the average moving speed of the auxiliary robot increases with the increase of the current frequency.

Secondly, we did three experiments to compare the kinematic performance of the guidance robot and the auxiliary robot. According to the data measured in the experiment, the error in the process of robot movement is obtained according to the average difference formula, and the curves shown in Figs. 19, 20, 21, and 22 are made. As can be seen from these four figures,

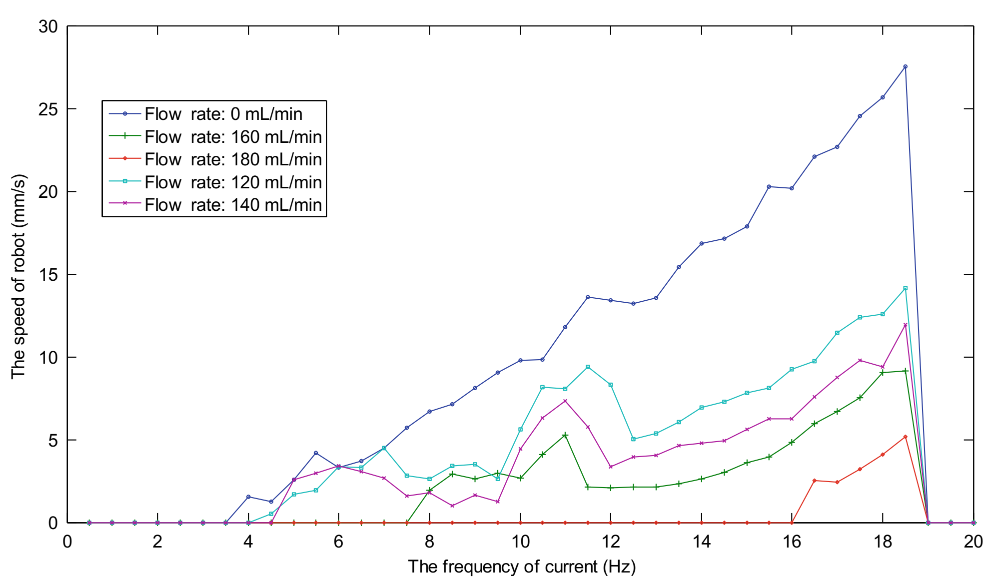

Fig. 16 The relationship between the frequency of the current signal and the average moving speed of the guide robot when it moves upstream backward under different flow velocities

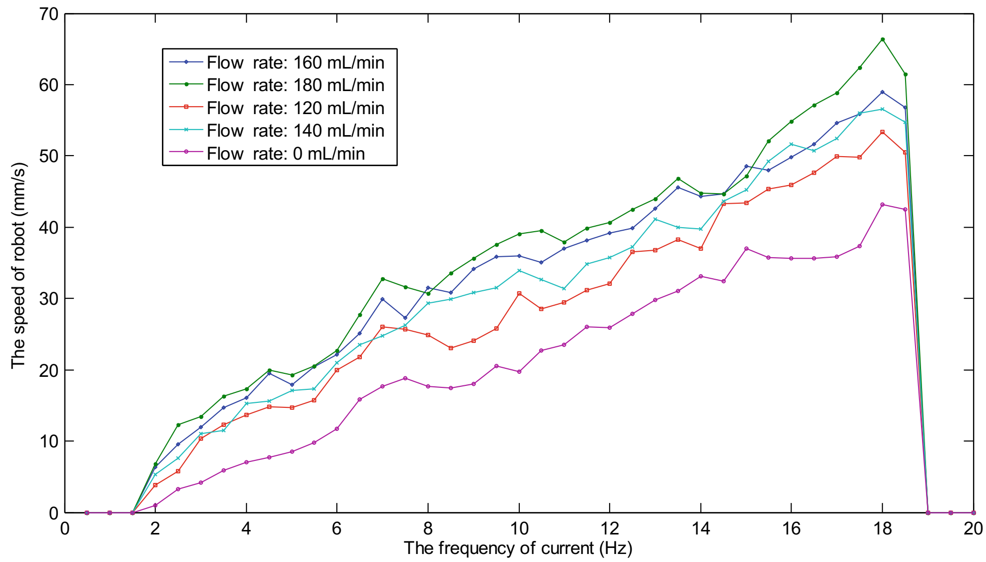

Fig. 17 The relationship between the frequency of the current signal and the average moving speed of the auxiliary robot when it moves downstream forward under different flow velocities

the error in the forward flow is generally greater than the error in the reverse flow, and the error under low-speed movement is generally smaller than the error under high-speed movement. When the frequency is higher than 14 Hz, the movement speed of the robot fluctuates greatly. Therefore, when applying the robot to practice, the robot should be controlled below 14 Hz to achieve stable movement. At the same time, the speed-increasing error of the auxiliary robot has almost no large fluctuations in the entire working frequency. In the above analysis, the influence of the guided robot tail modular interface on kinematic performance was also verified.

Thirdly, in order to show the robot's movement performance more realistically, we conducted the movement experiments of the capsule robot in the bent tube and in the fresh pig intestine. The movement of the robot is controlled wirelessly by the joystick.

Figure 23 a and b show the snapshots of the movement of the guide robot and the auxiliary robot under a curved pipe with a curvature of 11, respectively.

Figures 24 and 25 show the relationship between the current frequency and the average forward speed of the guide robot and the auxiliary robot at different curvatures, respectively. As the turning movement was controlled manually, the error of each measurement could not control very well. So, its speed of movement had certain fluctuations. However, it can still be concluded from the figure that the performance of the two robots in the curved pipe is slightly lower than that in the straight pipe, but the normal movement can still be guaranteed. This experiment validates the effectiveness of robot turning motion control in this system.

In order to increase the persuasion of the experiment and further verify the motion performance and image information

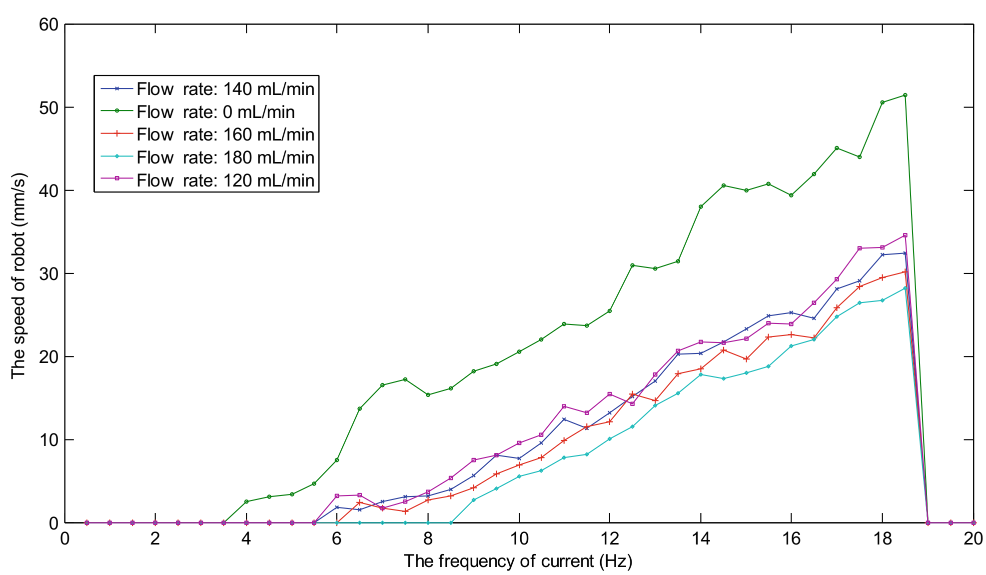

Fig. 18 The relationship between the frequency of the current signal and the average moving speed of the auxiliary robot when it moves downstream backward under different flow velocities

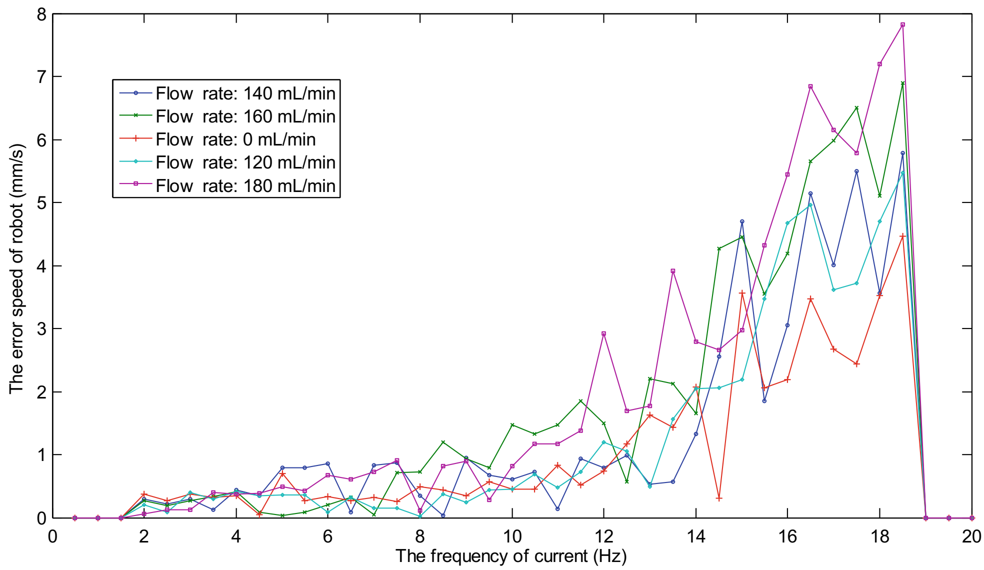

Fig. 19 The relationship between the frequency of the current signal and the average moving speed error of the guide robot when they move downstream forward under different flow velocities

acquisition function of the capsule robot proposed in this subject, this study designed and conducted the performance evaluation test of the capsule robot under the environment of pig large intestine. The experiment selected a fresh pig large intestine with a length of 25 cm. The fresh pig large intestine without water injection is shown in Fig. 26. The fresh pig large intestine after water injection is shown in Fig. 27.

Since the pig's large intestine is not transparent, it is impossible to observe the motion process of the capsule robot intuitively. Therefore, we attached a luminous body to the front of the robot and set up the experimental environment under the condition of insufficient light. The position of the capsule robot depends on the position of the capsule robot light body. Several snapshots of the capsule robot's movement were taken, as shown in Fig. 28. The entire process is 20 s. It can be seen from Fig. 28. The robot can move back and forth in the pig's large intestine.

Finally, we carried out the rendezvous and separation experiments of modular capsule robots. By comparing the data in Figs. 15, 16, 17, and 18, it can be concluded that the difference between the forward and backward speed of the guide robot is relatively large. So, we can take advantage of this feature by allowing the guide robot to move backward slowly and the auxiliary robot to move forward fast until they achieve rendezvous action. Then, by reversing the direction of the magnetic field, the guide robot and the auxiliary robot move counter to each other to achieve the separation action.

Figure 29 is the snapshot of rendezvous and separation of the guide robot and auxiliary robot with a flow velocity of 0 in a straight tube. The figure shows that the guide

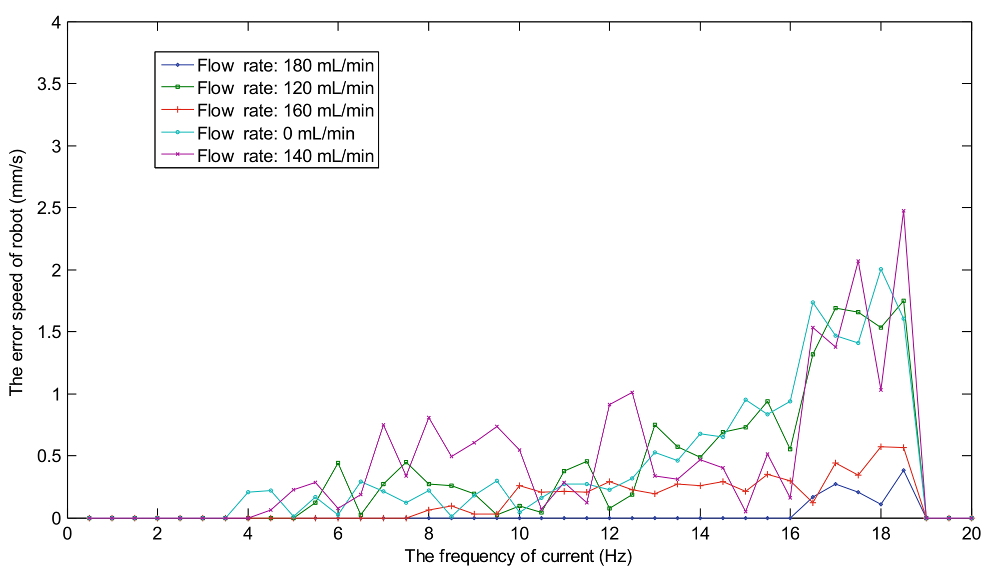

Fig. 20 The relationship between the frequency of the current signal and the average moving speed error of the guide robot when they move downstream backward under different flow velocities

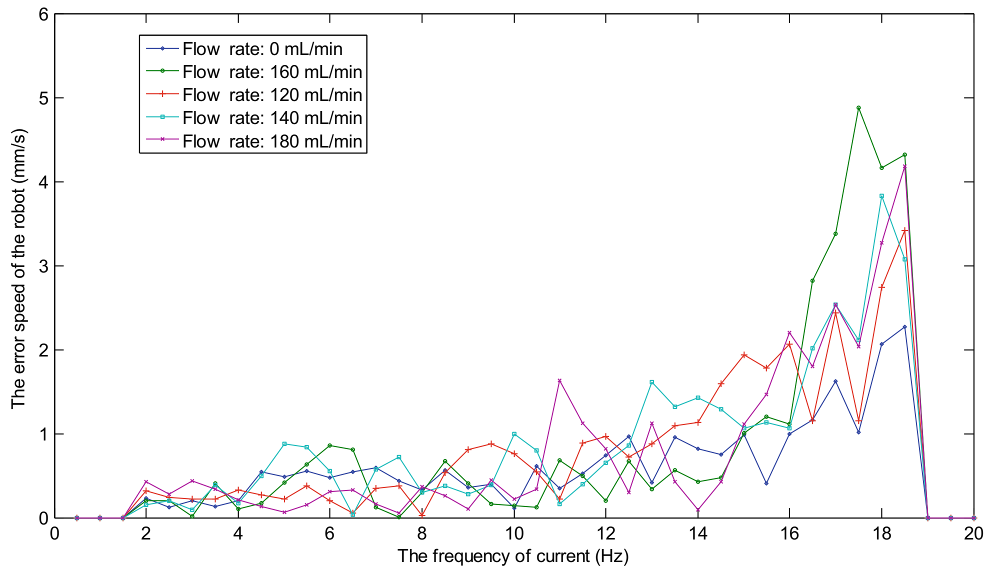

Fig. 21 The relationship between the frequency of the current signal and the average moving speed error of the auxiliary robot when they move downstream forward under different flow velocities

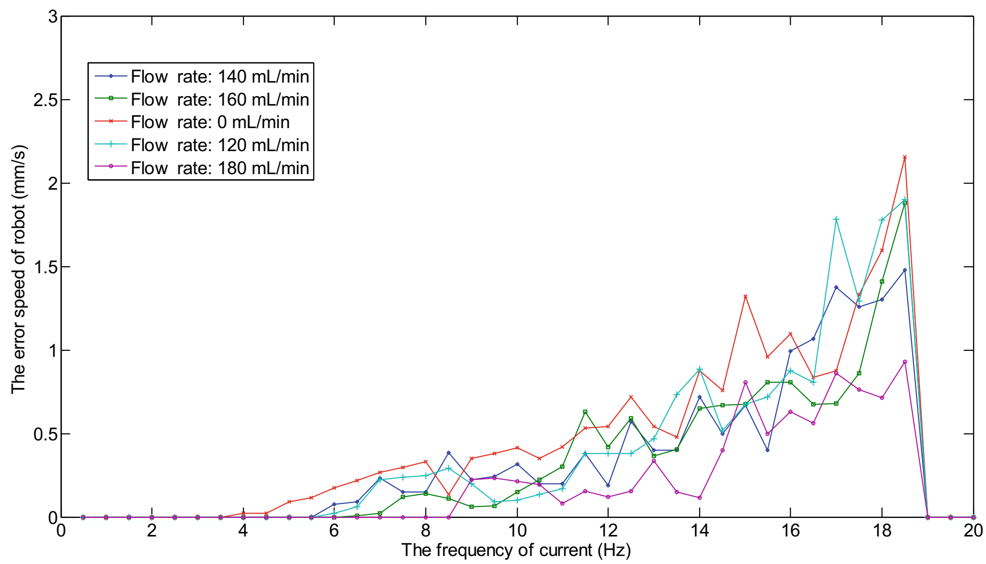

Fig. 22 The relationship between the frequency of the current signal and the average moving speed error of the auxiliary robot when they move downstream backward under different flow velocities

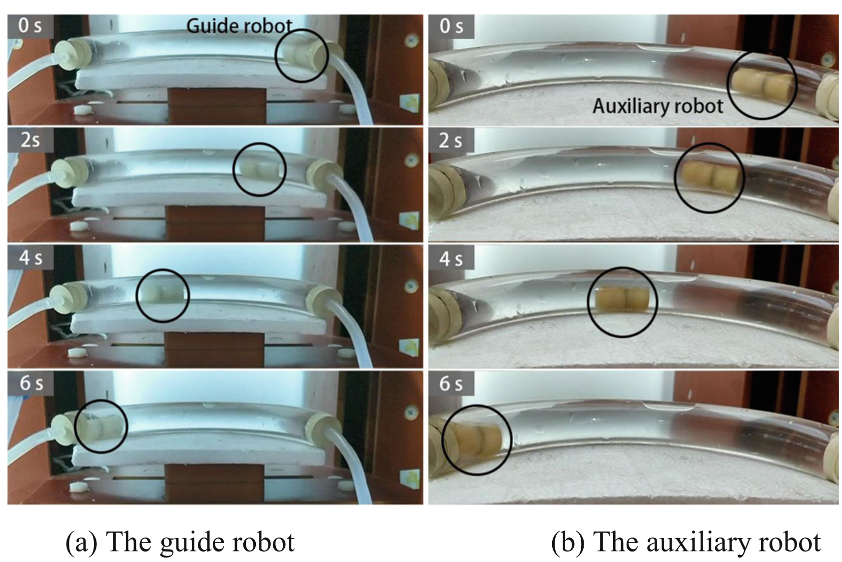

Fig. 23 The snapshots of the movement of the guide robot and the auxiliary robot under a curved pipe with a curvature of 11. **a** The guide robot. **b** The auxiliary robot

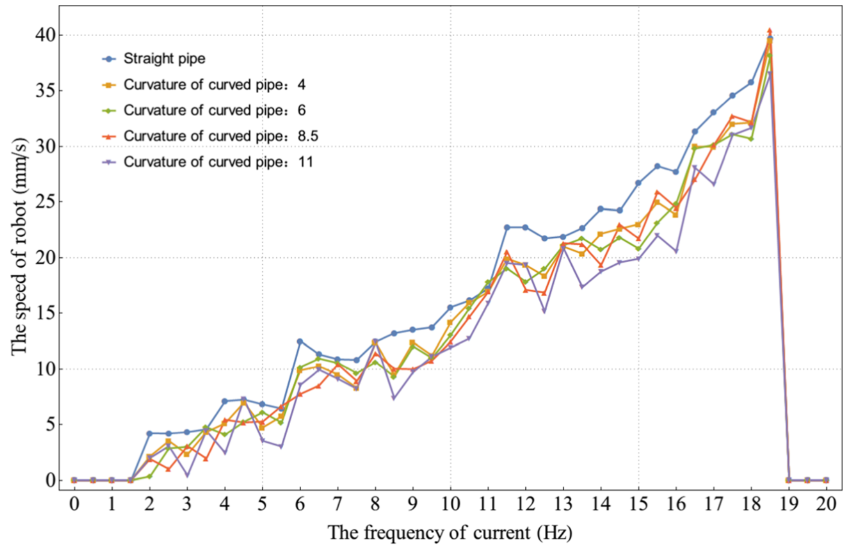

Fig. 24 The relationship between the current frequency and the average forward speed of the guide robot at different curvatures

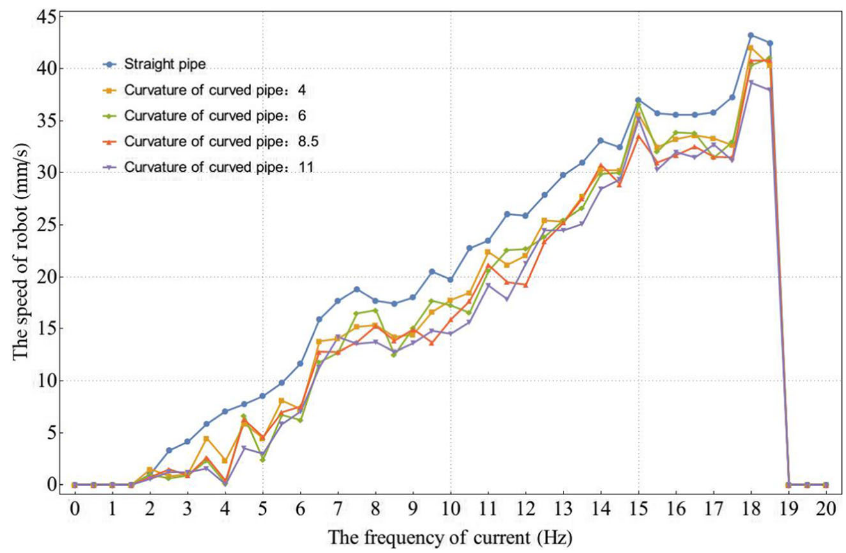

Fig. 25 The relationship between the current frequency and the average forward speed of the auxiliary robot at different curvatures

robot and the auxiliary robot move toward each other when the flow velocity is 0. Until rendezvous, the guide robot moved 35 mm backward, and the auxiliary robot moved 80 mm forward. Then they successfully implement the separation action [31].

Figure 30 shows the snapshot of rendezvous and separation of the guide robot and auxiliary robot with a flow velocity of 160 mL/min in a straight tube. It can be seen from the figure that the guide robot moved only 5 mm backward before rendezvous. This experiment validated the effectiveness of

Fig. 26 The fresh pig large intestine without water injection

Fig. 27 The fresh pig large intestine after water injection

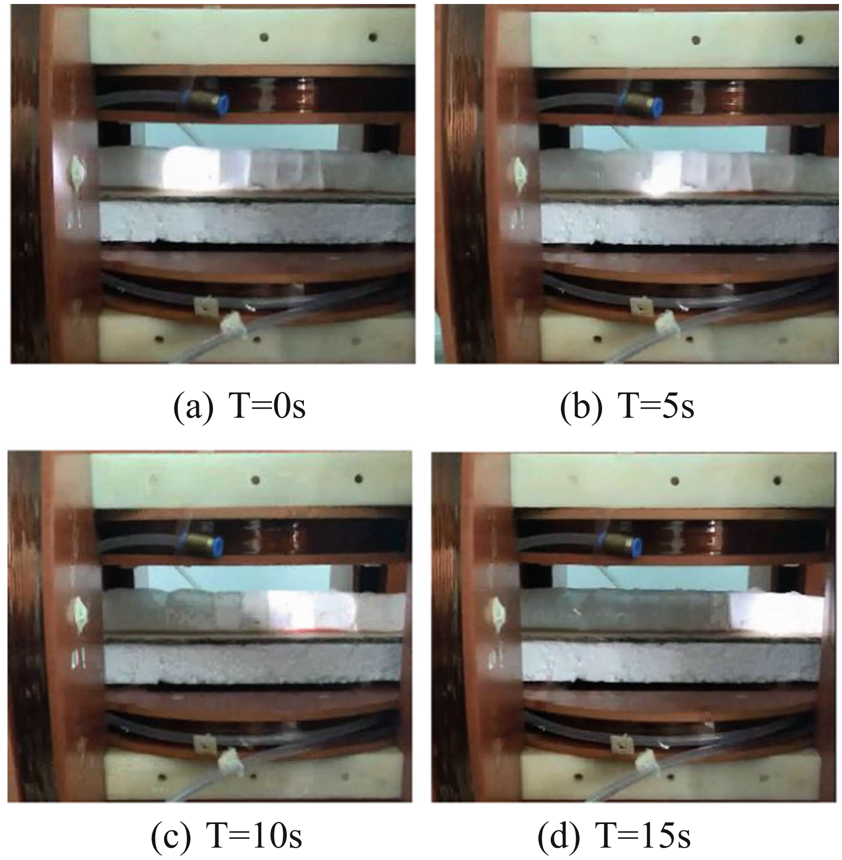

Fig. 28 The snapshots of the motion process of the capsule robot. **a** $T = 0$ s. **b** T = 5 s. **c** $T = 10$ s. **d** $T = 15$ s

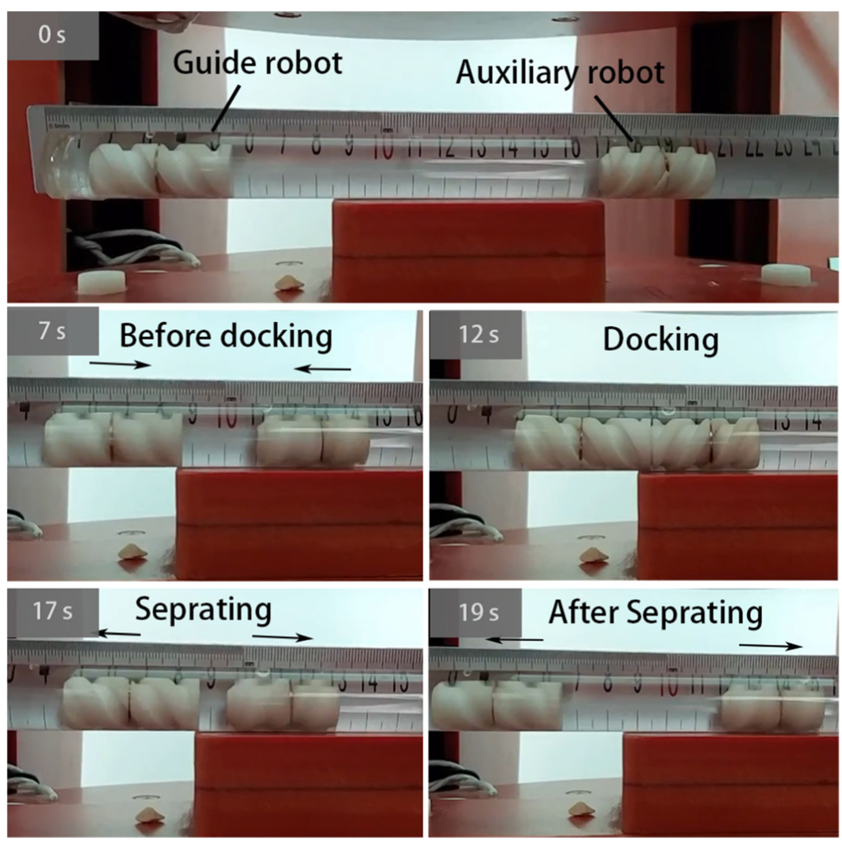

Fig. 29 The snapshot of rendezvous and separation of the guide robot and auxiliary robot with a flow velocity of 0 in a straight tube

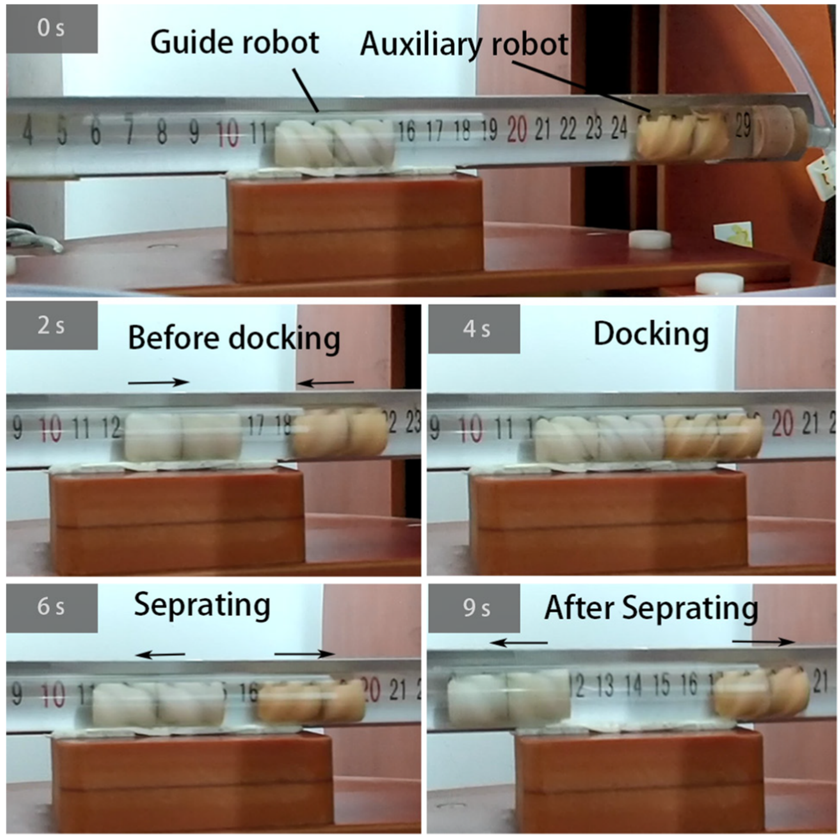

Fig. 30 The snapshot of rendezvous and separation of the guide robot and auxiliary robot with a flow velocity of 160 mL/min in a straight tube

modularity of the modular capsule robotic system and provided theoretical support for practical clinical applications.

5 Conclusions

In this paper, we proposed a novel wireless modular capsule robotic system. The system realized the motion control of the modular capsule robot in the pipe through the three-dimensional rotating magnetic field generated by the three-axis Helmholtz coils. The modular capsule robots can move forward and backward in the pipe in the axial direction, turn in a bending environment, and achieve the rendezvous and separation action. The proposed modular capsule robots include two units: the guide and the auxiliary robot. The helical guide grooves on the two robots rotate in the opposite direction, so the opposite axial movement can be carried out under the same rotating magnetic field. The rear of the guide robot and the head of the auxiliary robot are designed with a modular interface, which can achieve the rendezvous function with the embedded magnet at close distances and the separation action when they moving in the opposite direction. In addition, we have also designed a power supply control system to control the movement of the proposed robots. We also carried out a series of experiments to verify the dynamic model of the robot in the fluid. The experiments include evaluating the movement characteristics of the robots moving forward and backward in the environment of imitation of the human digestive tract, the performance difference between the guide robot and the auxiliary robot, and the motion characteristics in the bending environment. Finally, we carried out the rendezvous and separation experiments between the guide and auxiliary robots. The effectiveness of the modularity of the modular capsule robotic system has been validated. In the future, we will add some additional features to the robot and conduct the appropriate in vivo experiments.

In future research, the research team will place the image acquisition module on the main robot to make it have diagnostic functions, while the auxiliary robot will carry out targeted drug delivery. The functions and functions of the biopsy will enable the two robots not only to move independently to realize their respective functions but also to coordinate the functions of diagnosis and treatment. In vivo experiments will also be conducted, hoping to carry out experiments in vivo and apply all the functions of the robot in vivo.

Funding information This research is supported by the Natural Science Foundation of Tianjin (18JCYBJC43200) and Tianjin Key Laboratory for Control Theory and Application in Complicated Systems (TJKL-CTACS-201903) and Innovative Cooperation Project of Tianjin Scientific and Technological Support (18PTZWHZ00090).

References

1. Gavriel I, Gavriel M, Arkady G et al (2000) Wireless capsule endoscopy [J]. Nature 405(6785):417–417
2. Andrea M, Arianna M, Paolo D et al (2009) Capsule endoscopy: progress update and challenges ahead [J]. Nat Rev Gastroenterol Hepatol 6(6):353–361
3. Marco Q, Arianna M, Sergio S et al (2008) Design and fabrication of a motor legged capsule for the active exploration of the gastrointestinal tract [J]. IEEE/ASME Trans Mechatronics 13(2):169–179
4. Gao P, Guozheng Y, Wang Z et al (2011) A robotic endoscope based on minimally invasive locomotion and wireless techniques for human colon [J]. Int J Med Robot Comput Assist Surg 7(3): 256–267
5. Zhen-Jun S, Bo Y, Yang Q et al (2014) Preliminary study of a legged capsule robot actuated wirelessly by magnetic torque [J]. IEEE Trans Magn 50(8):1–6
6. Koga H, SAKATA Y, Hirose S, et al. Capsule microrobot for targeting in medical diagnostic treatment [C]. Solid-state sensors, actuators and microsystems conference (TRANSDUCERS), 2011 16th International. IEEE, 2011: 2835–2838.
7. Wen-Wen C, Guo-Zheng Y, Hua L et al (2014) Design of micro biopsy device for wireless autonomous endoscope [J]. Int J Precis Eng Manuf 15(11):2317–2325
8. Choi K, Jang G, Jeon S et al (2014) Capsule-type magnetic microrobot actuated by an external magnetic field for selective drug delivery in human blood vessels [J]. IEEE Trans Magn 50(11):1–4
9. Hoon KS, Kazushi I (2014) Magnetic robot and manipulation for active-locomotion with targeted drug release [J]. IEEE/ASME Trans Mechatronics 19(5):1651–1659
10. Yu M (2002) M2ATM capsule endoscopy: a breakthrough diagnostic tool for small intestine imaging [J]. Gastroenterol Nurs 25(1): 24–27
11. Sehyuk Y, Metin S (2012) Design and rolling locomotion of a magnetically actuated soft capsule endoscope [J]. IEEE Trans Robot 28(1):183–194
12. Sehyuk Y, Metin S (2012) Shape-programmable soft capsule robots for semi-implantable drug delivery [J]. IEEE Trans Robot 28(5): 1198–1202
13. Sehyuk Y, Kartik G, Metin S (2013) Magnetically actuated soft capsule with the multimodal drug release function [J]. IEEE/ ASME Trans Mechatronics 18(4):1413–1418
14. Wenwen C, Guozheng Y, Wang Z et al (2014) A wireless capsule robot with spiral legs for human intestine [J]. Int J Med Robot Comput Assist Surg 10(2):147–161
15. He S, Guozheng Y, Gao J et al (2015) Frictional and viscous characteristics of an expanding-extending robotic endoscope in the intestinal environment [J]. Tribol Lett 58(3):36
16. Yongshun Z, Shengyuan J, Xuewen Z et al (2011) A Variable-diameter capsule robot based on multiple wedge effects [J]. IEEE/ ASME Trans Mechatronics 16(2):241–254
17. Zhang Yongshun, Xie Huaying, Wang Na, et al. Design, analysis and experiments of a spatial universal rotating magnetic field system for capsule robot [C]. 2012 IEEE International Conference on Mechatronics and Automation, 2012: 998–1003.
18. Yongshun Z, Wang N, Chunyu D et al (2013) Control theorem of a universal uniform-rotating magnetic vector for capsule robot in curved environment [J]. SCIENCE CHINA Technol Sci 56(2): 359–368
19. Yongshun Z, Jianwei B, Minglu C et al (2014) Optimal control of a universal rotating magnetic vector for petal-shaped capsule robot in curve environment [J]. sChin J Mech Eng 5(27):880–889
20. Yongshun Z, Zhongkan S, Minglu C et al (2016) Magnitude and orientation error correction of a superimposed spatial universal rotating magnetic vector [J]. IEEE Trans Magn 52(5):1–9
21. YongShun Z, Yu ZC, Yang HY et al (2017) Orthogonal transformation operation theorem of a spatial universal uniform rotating magnetic field and its application in capsule endoscopy [J]. SCIENCE CHINA Technol Sci 60(6):854–864
22. Guo Shuxiang, Fu Qiang, Yamauchi Yasuhiro, et al. Characteristic evaluation of a wireless capsule microrobotic system [C]. 2013 IEEE International Conference on Mechatronics and Automation, 2013: 831–836.
23. Qiang F, Guo S, Yasuhiro Y et al (2015) A novel hybrid microrobot using rotational magnetic field for medical applications [J]. Biomed Microdevices 17(2):31
24. Qiang F, Guo S, Songyuan Z et al (2015) Characteristic evaluation of a shrouded propeller mechanism for a magnetic actuated microrobot [J]. Micromachines 6(9):1272–1288
25. Qiang F, Guo S, Qiang H et al (2016) Development and evaluation of novel magnetic actuated microrobot with spiral motion using electromagnetic actuation system [J]. J Med Biol Eng 36(4):506–514
26. Fu Q, Zhang S, Guo S, Guo J (2018) Performance evaluation of a magnetically actuated capsule microrobotic system for medical applications [J]. Micromachines 9(12):641
27. Liang Nan, Guo Jian, Guo Shuxiang, et al. Performance evaluation of the wireless micro robot in the fluid [C]. 2015 IEEE International Conference on Mechatronics and Automation, 2015: 958–963.
28. Guo Shuxiang, Liang Nan, Guo Jian, et al. Movement characteristics evaluation of the spherical robot actuated by the magnetic field for medical applications [C]. 2016 IEEE International Conference on Mechatronics and Automation, 2016: 448–453.
29. Ji-Yoon K, Yong-Cheol K, Yeh-Sun H (2012) Automated alignment of rotating magnetic field for inducing a continuous spiral motion on a capsule endoscope with a twistable thread mechanism [J]. Int J Precis Eng Manuf 13(3):371–377
30. Dey N, Ashour AS, Shi F, Sherratt RS (2017) Wireless capsule gastrointestinal endoscopy: direction-of-arrival estimation based localization survey. IEEE Rev Biomed Eng 10:2–11
31. Guo J, Liu P, Guo S et al (2017) Development of a novel wireless spiral capsule robot with modular structure [C]//2017 IEEE International Conference on Mechatronics and Automation (ICMA). IEEE:439–444
32. Filip D, Yadid-Pecht O, Andrews CN, Mintchev MP (2011) Self-stabilizing colonic capsule endoscopy: pilot study of acute canine models. IEEE Trans Med Imaging 30(12): 2115–2125
33. Zhang Kai. Research on driving and swimming characteristic of a capsule micro robot [D]. Dalian University of Technology, 2005.

Jian Guo received the B.S. degree in Information and Computing Science from the Changchun University of Technology, Jilin, China, in 2005 and the M.S. and the Ph.D. degrees from intelligent machine system from Kagawa University, Japan, in 2009 and in 2012, respectively. He is currently a full professor in Tianjin University of Technology, Tianjin, China. He has published about forty refereed journal and conference papers in recent three years. His current research is on biomedical robots, such as wireless microrobots in pipe and robotic catheter systems for biomedical applications. Dr. Guo received Best Conference Paper Award of CME 2013 and IEEE ICIA 2014 in 2013 and in 2014, respectively.

Zihong Bao received the B.S. degree in School of Electrical and Electronic Engineering from Tianjin University of Technology in 2017. Currently, he is working toward the M.S degree in Control Science and Engineering at Tianjin University of Technology, Tianjin, China. He has published 2 refereed conference papers.

Qiang Fu received the B.Sc. degree from the Harbin University of Science and Technology, Harbin, China, in 2010, and the M.S. and the Ph.D. degrees in Intelligent Machine System from Kagawa University, Japan, in 2014 and in 2017, respectively. He is currently an associate professor in Tianjin University of Technology, Tianjin, China. His current research is on biomedical robots, such as the development of multi-module magnetic actuated microrobotic systems for biomedical applications.

Shuxiang Guo (SM'03) received the Ph.D. degree in Mechano-informatics and Systems from Nagoya University, Japan, in 1995. He is currently a full professor at the Faculty of Engineering and Design, Kagawa University, Japan. He received the Chang Jiang Professor-ship Award from the Ministry of Education of China, in 2005, and he was offered Thousand-Elite-Project in China. He has published about four hundred refereed journal and conference papers. His current research includes biomimetic under-water robots and medical robot systems for minimally invasive surgery, microcatheter system, micropump, and smart material (SMA, IPMC) based on actuators. Dr. Guo is Editor in chief for the *International Journal of Mechatronics and Automation*.